ACS central science

http://pubs.acs.org/journal/acscii

Research Article

An Epoxide Intermediate in Glycosidase Catalysis

Lukasz F. Sobala,[¶] Gaetano Speciale,[¶] Sha Zhu,[¶] Lluís Raich,[¶] Natalia Sannikova, Andrew J. Thompson, Zalihe Hakki, Dan Lu, Saeideh Shamsi Kazem Abadi, Andrew R. Lewis, Víctor Rojas-Cervellera, Ganeko Bernardo-Seisdedos, Yongmin Zhang, Oscar Millet, Jesús Jiménez-Barbero, Andrew J. Bennet,* Matthieu Sollogoub,* Carme Rovira,* Gideon J. Davies,* and Spencer J. Williams*

Cite This: *ACS Cent. Sci.* 2020, 6, 760–770

Read Online

ACCESS | Metrics & More | Article Recommendations | Supporting Information

ABSTRACT: Retaining glycoside hydrolases cleave their substrates through stereochemical retention at the anomeric position. Typically, this involves two-step mechanisms using either an enzymatic nucleophile via a covalent glycosyl enzyme intermediate or neighboring-group participation by a substrate-borne 2-acetamido neighboring group via an oxazoline intermediate; no enzymatic mechanism with participation of the sugar 2-hydroxyl has been reported. Here, we detail structural, computational, and kinetic evidence for neighboring-group participation by a mannose 2-hydroxyl in glycoside hydrolase family 99 *endo*-α-1,2-mannanases. We present a series of crystallographic snapshots of key species along the reaction coordinate: a Michaelis complex with a tetrasaccharide substrate; complexes with intermediate mimics, a sugar-shaped cyclitol β-1,2-aziridine and β-1,2-epoxide; and a product complex. The 1,2-epoxide intermediate mimic displayed hydrolytic and transfer reactivity analogous to that expected for the 1,2-anhydro sugar intermediate supporting its catalytic equivalence. Quantum mechanics/molecular mechanics modeling of the reaction coordinate predicted a reaction pathway through a 1,2-anhydro sugar via a transition state in an unusual flattened, envelope (E_3) conformation. Kinetic isotope effects (k_{cat}/K_M) for anomeric-^{2}H and anomeric-^{13}C support an oxocarbenium ion-like transition state, and that for C2-^{18}O (1.052 ± 0.006) directly implicates nucleophilic participation by the C2-hydroxyl. Collectively, these data substantiate this unprecedented and long-imagined enzymatic mechanism.

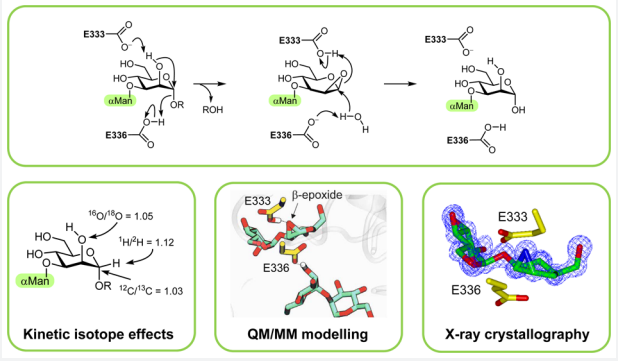

INTRODUCTION

Glycoside hydrolases (glycosidases) catalyze the transfer of the glycosyl group of glycosides to water or another nucleophilic molecule.[1] One major group of glycosidases are those that cleave their glycoside substrates with a net retention of anomeric configuration. Retaining glycosidases typically operate through two-step mechanisms involving a covalent glycosyl enzyme intermediate formed from a nucleophilic amino acid residue (Asp, Glu, or Tyr) (Figure 1a). Alternatively, certain retaining hexosaminidases act through a mechanism involving neighboring-group participation by the 2-acetamido (or glycolylamido) group of the substrate.

While there is extensive evidence for neighboring-group participation by a 2-acetamido group in hexosaminidases, these are the only glycosidases for which neighboring-group participation is accepted. Interestingly, there is a large body of evidence supporting neighboring-group participation by a glycoside 2-hydroxyl in the alkaline cleavage of 1,2-*trans*-glycosides and glycosyl fluorides and 1,2-anhydro sugars (a 1,2-epoxide) as intermediates. These data include the well-known differences in the rate of alkaline hydrolysis of 1,2-*cis*- versus 1,2-*trans*-glycosides, the reduced rate of alkaline hydrolysis of otherwise identical 2-alkylated 1,2-*trans*-glycosides,[2] and retention of anomeric stereochemistry in the alkaline methanolysis of 1,2-*trans*-glycosyl fluorides whereas 2-alkylated 1,2-*trans*-glycosyl fluorides react with inversion.[3] Kinetic isotope effects for the alkaline hydrolysis of 4-nitrophenyl α-D-mannopyranoside have given direct evidence for neighboring-group participation by a C2-oxyanion.[4] Neighboring-group participation by a 2-hydroxyl has also been proposed for other glycoside hydrolases,[5,6] but none have withstood cursory, let alone detailed, mechanistic scrutiny.[7−9]

Glycosidases of CAZY (see www.cazy.org; www.cazypedia.org)[10,11] family 99 are *endo*-acting retaining enzymes that cleave α-mannosidic linkages within α-mannans in the yeast cell wall (*endo*-α-1,2-mannanases)[12] and mammalian glucosylated high-mannose N-glycans (*endo*-α-1,2-mannosi-

Received: January 31, 2020
Published: April 16, 2020

https://dx.doi.org/10.1021/acscentsci.0c00111
ACS Cent. Sci. 2020, 6, 760–770

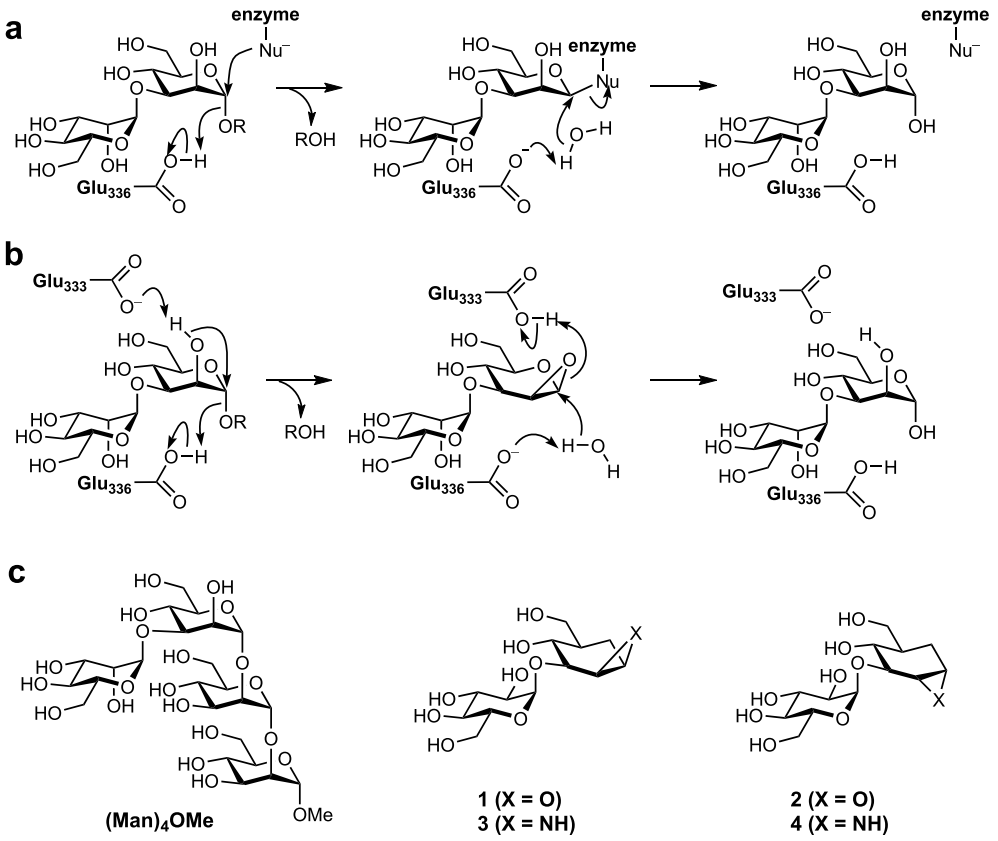

Figure 1. Proposed mechanisms for a retaining glycoside hydrolase applied to a GH99 *endo*-α-1,2-mannanase. (a) Classical Koshland mechanism involving an enzymatic nucleophile and a glycosyl enzyme intermediate. Residue numbering is for *Bt*GH99. (b) Alternative mechanism involving neighboring-group participation by the 2-hydroxy group and a 1,2-anhydro sugar intermediate. (c) Structures of ligands used in this study.

dases).[13−15] These enzymes have important roles in fungal cell wall degradation in the human gut microbiota[16] as well as processing of glucosylated intermediates in N-glycan biosynthesis,[17] respectively. For both types of enzyme, the minimum substrate is a disaccharide in which the reactive, −1 mannosyl residue is modified at the 3-position with either an α-mannosyl or α-glucosyl residue. The first X-ray structures of members of GH family 99, *endo*-α-1,2-mannanases from *Bacteroides thetaiotaomicron* and *Bacteroides xylanisolvens*, *Bt*GH99 and *Bx*GH99, respectively, provided hints of an atypical mechanism.[18] These bacterial representatives act on both α-glucosyl- and α-mannosyl-1,3-α-mannosides (with around 10-fold preference for the latter), and structural studies using substrate-like ligands were applied to identify the enzymatic catalytic machinery. However, 3-dimensional structures of wild-type *Bt*GH99 in complex with the isofagomine-derived inhibitors GlcIFG[18] and ManIFG,[12] and a disabled non-catalytic mutant in complex with a substrate,[12] failed to identify a likely enzymatic nucleophile appropriately situated near the fissile anomeric bond. Enticingly, complexes with deoxymannojirimycin-derived inhibitors GlcDMJ[18] and Man-2-amino-DMJ,[19] noeuromycin-derived inhibitors GlcNOE[18] and ManNOE,[20] and of the E333Q mutant with substrate,[12] highlighted an interaction between a carboxylate residue and the 2-hydroxyl of the −1 mannosyl residue. Collectively, these data were suggestive of an alternative mechanism involving a 1,2-anhydro sugar intermediate (Figure 1b); however, no studies have provided direct evidence for participation of O2 or insight into the proposed epoxide intermediate.

Here, we present an analysis of the reaction mechanism of GH99 *endo*-α-1,2-mannanases. X-ray data of molecular probes, designed to mimic species along the reaction coordinate, provide a snapshot of key catalytic states. These results are extended by applying quantum mechanics/molecular mechanics (QM/MM) methods to study the enzyme-catalyzed reaction, giving computational support for the formation of a 1,2-anhydro sugar intermediate. We also show that a cyclitol epoxide mimic of the 1,2-anhydro sugar exhibits reactivity that is consistent with the expected reactivity of this intermediate. Finally, we measure kinetic isotope effects that provide direct experimental support for neighboring-group participation by the substrate 2-hydroxy group in *Bt* and *Bx*GH99.

RESULTS

Structures of the "Michaelis" and Product Complexes of *Bx*GH99. As a first step in the mechanistic dissection of GH99 enzymes, and to provide structural data for computational approaches to study the reaction coordinate, we sought to define, at near atomic resolution, the two ends of the reaction coordinate. We thus determined substrate ("Michaelis") and product complexes of *Bx*GH99. A catalytically inactive variant, E333Q, was used to obtain a complex with the substrate $(Man)_4OMe$ (representing a fragment of the yeast mannan that is the substrate for this bacterial enzyme),[12] at a resolution of 1.07 Å (Figure 2a; for X-ray data collection and refinement statistics, see Table S1). The intact tetrasaccharide occupies the −2 to +2 subsites,[21] spanning the active site.

https://dx.doi.org/10.1021/acscentsci.0c00111
ACS Cent. Sci. 2020, 6, 760−770

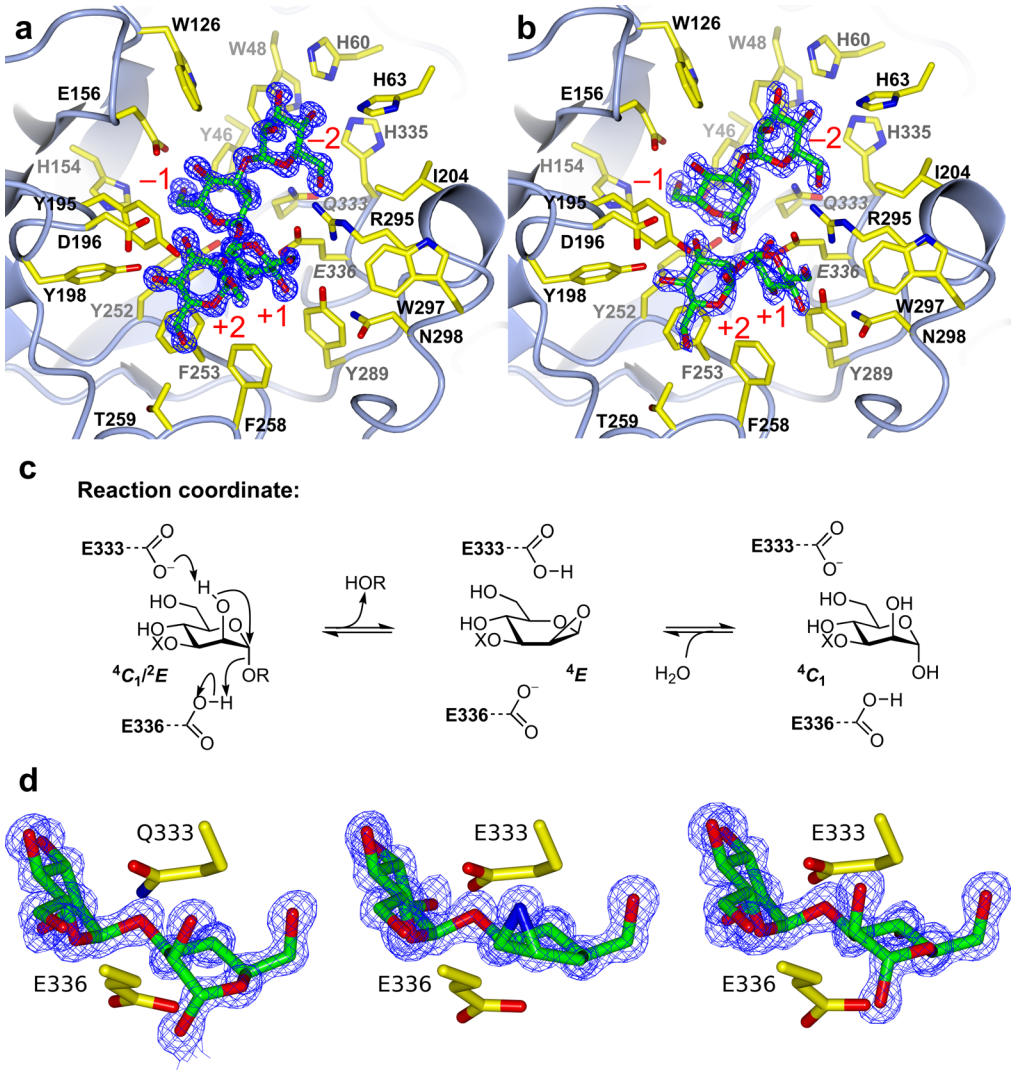

Figure 2. X-ray snapshots along the *Bx*GH99 reaction coordinate. X-ray structures of (a) *Bx*GH99-E333Q bound to αMan-1,3-αMan-1,2-αMan-1,2-αMan-OMe [$(Man)_4OMe$]; (b) *Bx*GH99-E333Q bound to α-1,3-mannobiose and α-1,2-mannobiose. Key catalytic active site residues in italics. (c) Proposed reaction coordinate of the GH99-catalyzed reaction (X = αMan). (d) X-ray structures showing the −2/−1 subsites for the Michaelis complex, *Bx*GH99-E333Q with $(Man)_4OMe$; intermediate complex, wild-type with cyclohexane β-1,2-aziridine **3**; and product complex, α-1,3-mannobiose and α-1,2-mannobiose with wild-type. $2mF_0 - F_c$ weighted electron density maps contoured at 0.8 $e^-/Å^3$ in all cases.

Within the Michaelis complex, the −1 mannoside residue adopts a $^4C_1$ conformation that is slightly distorted toward ^2E; this distortion can be confidently assigned at the atomic resolution of the data. There is no major protein conformational change (indeed, none has been seen in any GH99 structure), and as seen in previous disaccharide and inhibitor complexes, no candidate enzymatic nucleophile is located near the reactive anomeric C1 carbon. Tyr252 is approximately 4 Å away from C1 in *Bx*GH99, and mutagenesis of the equivalent residue in human *endo*-α-mannosidase (39% sequence identity to *Bx*GH99) gave a mutant enzyme that maintained its ability to perform transglycosylation, excluding the possibility that this residue provides nucleophilic catalysis.[22] Of note is the interaction, 2.8 Å, between the Nε2 of the introduced Gln333 with the O2 of the −1 subsite mannoside. The natural Glu at this position is proposed to act as the catalytic base for the deprotonation of O2 during the formation of the 1,2-anhydro sugar intermediate (Figure 1b). The Michaelis complex shows that this residue is ideally placed, consistent with the complete loss of activity when Glu333 is substituted by Gln.[18]

The final enzyme-bound state of the reaction coordinate was determined through studies of product complexes. We solved ternary complexes of wild-type and E333Q variant *Bx*GH99 enzymes with the two products of hydrolysis: α-1,3-mannobiose and α-1,2-mannobiose, at 1.08 and 1.65 Å resolution, respectively. In both complexes, α-1,3-mannobiose is bound in the −2, −1 subsites, and α-1,2-mannobiose is bound in the +1, +2 subsites (Figure 2b, Figure S1). Comparison of the Michaelis and product complexes reveals that, in the latter complex, the −1 sugar is in a relaxed $^4C_1$ conformation, which is consistent with the lack of a covalent bond connecting the −2/−1 and +1/+2 sugars, and the +1 mannose residue is shifted, such that it makes different hydrogen bonds to the protein. Thus, in the substrate complex the +1 mannose O3 hydrogen bonds to E336 O1, whereas in the product complex O3 is hydrogen bonded with Y289, and a water molecule resides where O3 sat in the substrate. Similarly, in the substrate complex the +1 mannose O4 hydrogen bonds with water whereas in the product complex hydrogen bonds with the Y289 oxygen (see Figure S2).

https://dx.doi.org/10.1021/acscentsci.0c00111
ACS Cent. Sci. 2020, 6, 760−770

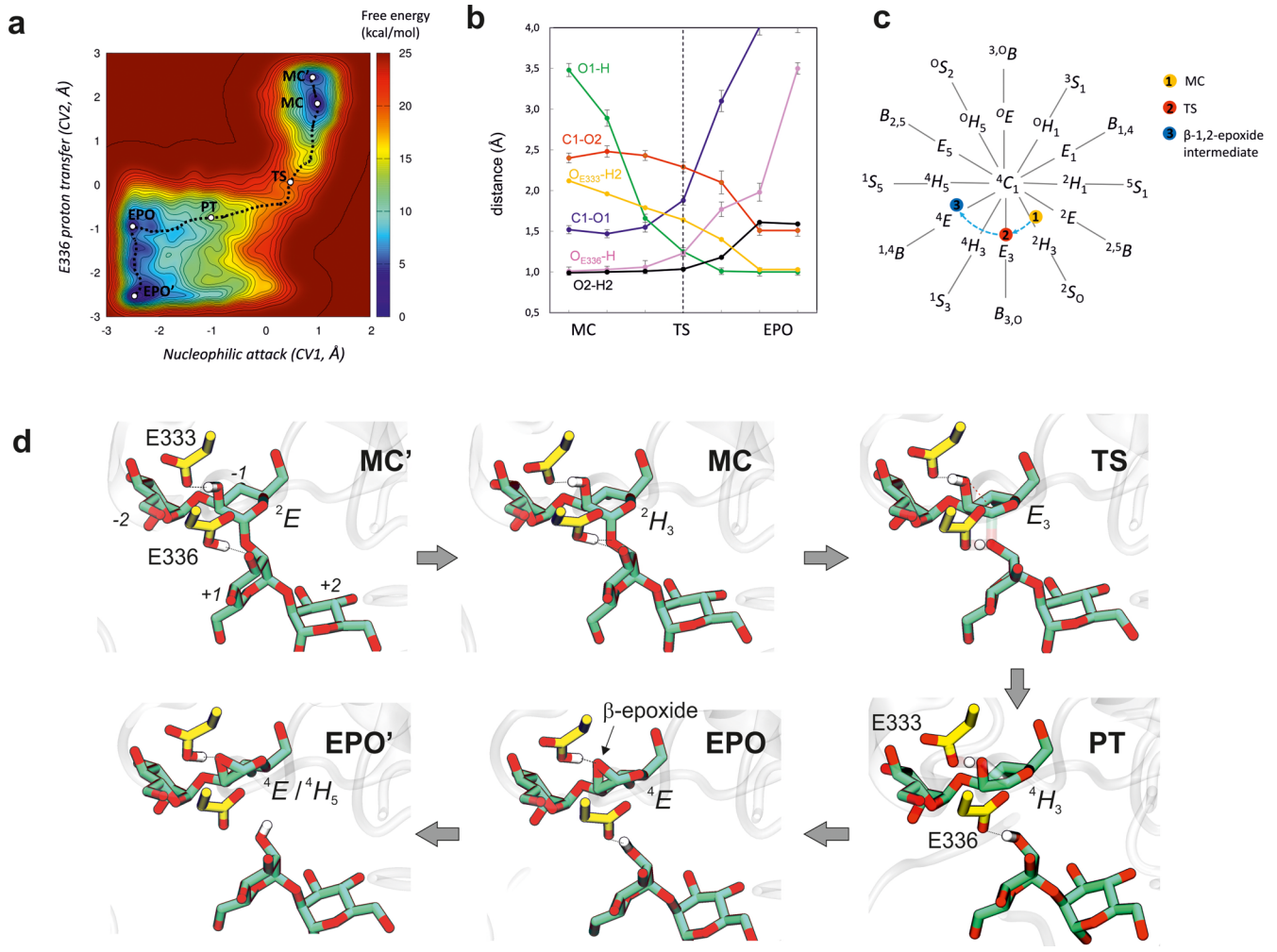

Figure 3. QM/MM metadynamics modeling of the *Bx*GH99 *endo*-α-1,2-mannanase catalyzed reaction. (a) Free energy landscape (FEL) of the enzymatic reaction with respect to the two collective variables described in the text. Contour lines are at 0.5 kcal/mol. (b) Evolution of relevant distances along the minimum free energy pathway (reaction coordinate). Averages over all configurations sampled for each point on the pathway are considered. Error bars correspond to standard deviations. (c) Conformational itinerary of the α-mannoside at the −1 subsite along the reaction coordinate projected into Stoddart's diagram. (d) Representative snapshots of the main states along the reaction coordinate (MC, MC′, Michaelis complexes; TS, transition state; PT, proton transfer; EPO, EPO′, 1,2-anhydro sugar.

Both the "Michaelis" and product complexes are thus consistent with a reaction mechanism involving neighboring-group participation by the substrate 2-hydroxy group, activated through deprotonation by Glu333 and with Glu336 acting as the catalytic acid for leaving group departure. Given this enticing structural support for this mechanism, we next sought to dissect the reaction coordinate using a computational approach.

QM/MM Metadynamics Simulations of the *endo*-α-1,2-Mannanase-Catalyzed Reaction. To probe the potential neighboring-group participation by the substrate 2-hydroxy group, we modeled the reaction mechanism of the *endo*-α-1,2-mannanase-catalyzed reaction using classical molecular dynamics (MD) and QM/MM metadynamics simulations (see the Supplementary Methods).[23,24] This approach accounts for the room temperature motion of the enzyme during the reaction while providing QM (DFT) accuracy for the description of the active site atoms. It has been used with success to model reaction mechanisms in a wide range of carbohydrate-active enzymes,[25] including Golgi α-mannosidase II.[26] Two collective variables (CVs) were used to define the reaction coordinate starting with the Michaelis complex, described above. These variables were chosen as to include the main bonds that are to be made/broken during the reaction (Figure 2c). The first collective variable (CV1, representing *nucleophilic attack*) was defined as the distance difference between C1−O1 and O2−C1. The second collective variable (CV2, *glycosidic bond protonation*) was defined as the distance difference between O1−H_{E336} and H_{E336}−O_{E336}.

The free energy landscape reconstructed from the simulation (Figure 3a,b) shows that the Michaelis complex evolves to the product via a 1,2-anhydro sugar intermediate. An energy barrier of $\Delta G^{\ddagger} \approx 15$ kcal/mol between the Michaelis complex (MC) and the transition state (TS) leads to the formation of a 1,2-anhydro sugar (EPO; local minimum on the right-hand-side). The computed free energy barrier is in good agreement with the available kinetic data;[16] the reaction is therefore both feasible and favored. The two minima located in the reactants region (MC and MC′) correspond to alternative arrangements of the Michaelis complex in which the O−H bond of the acid/base residue E336 twists to point toward either the glycosidic

https://dx.doi.org/10.1021/acscentsci.0c00111
ACS Cent. Sci. 2020, 6, 760−770

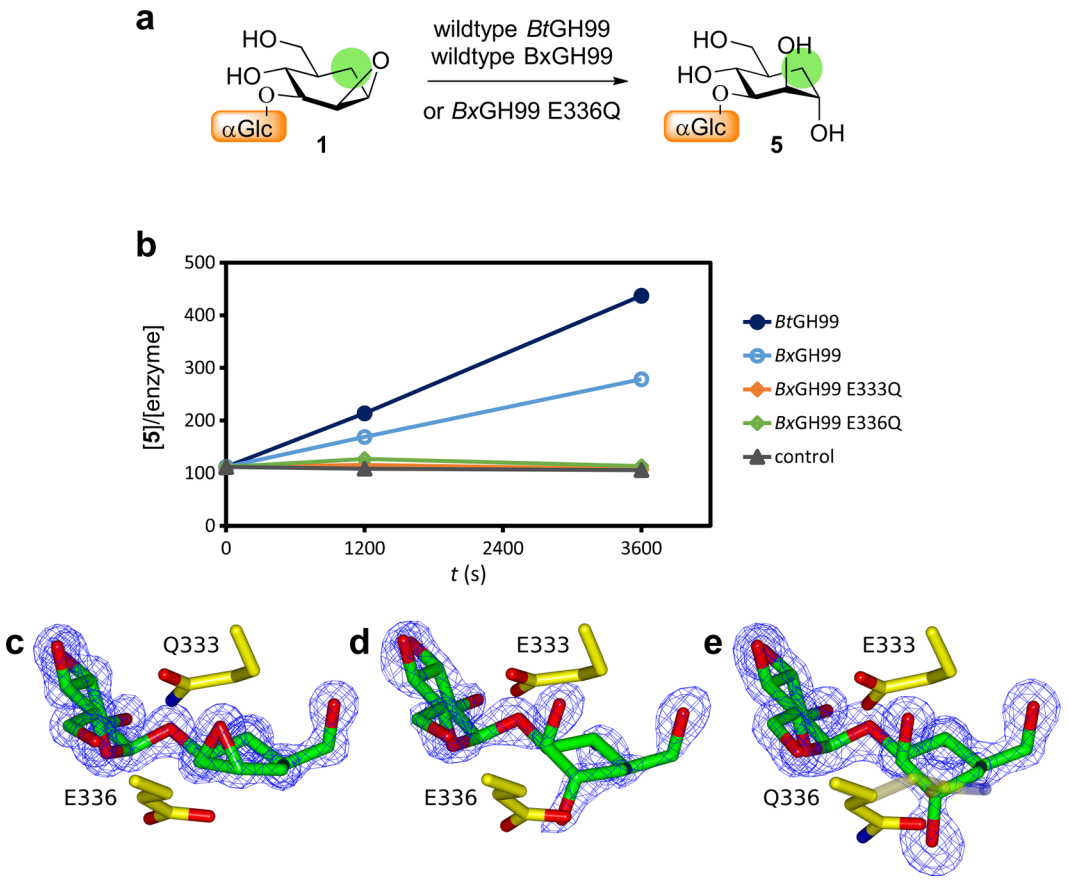

Figure 4. Structure and reactivity of cyclohexane β-1,2-epoxide **1**. (a) Enzyme-catalyzed reaction of cyclohexane β-1,2-epoxide. (b) Monitoring of enzyme-catalyzed reaction of cyclohexane β-1,2-epoxide by mass spectrometry with wild-type and E333Q and E336Q mutants. X-ray structures of (c) cyclohexane β-1,2-epoxide with *Bx*GH99 E333Q mutant ($2mF_o - DF_c$ at 0.8 $e^-/Å^3$); (d) hydrolysis product *trans*-1,2-diol with wild-type ($2mF_o - DF_c$ at 0.5 $e^-/Å^3$), and with (e) E336Q mutant ($2mF_o - DF_c$ at 0.5 $e^-/Å^3$).

oxygen or the +1 saccharide. The calculated TS is dissociative, with the glycosidic bond elongated (C1−O1 = 1.88 ± 0.06 Å; Figure 3b and Table S2) and the O2 atom at an early stage of attack on the anomeric carbon (C1−O2 = 2.29 ± 0.06 Å), causing weakening of the C2−O2 bond. Analysis of the structures along the reaction coordinate (Figure 3c,d) reveals distortion of the −1 mannosyl ring during the reaction, following a $^2E/^2H_3 \rightarrow [E_3]^{\ddagger} \rightarrow {}^4E$ itinerary during the first half of the reaction, which can be considered an "electrophilic migration" of C1 from the leaving group oxygen in the Michaelis complex, to the nucleophilic O2 in the EPO complex (Figure S3). The conformation of the MC ($^2E/^2H_3$) is similar to the one obtained from the X-ray structure (between $^4C_1$ and ^2E; see Figure S4), with only slight differences that can be attributed to the E333Q mutation in the X-ray structure altering the nature of the interaction of this residue with the substrate 2-OH. The conformation of the −1 mannosyl residue at the TS (E_3) achieves planarity of C2−C1−O−C5, as required for an oxocarbenium-ion-like transition state.[1] Finally, the calculated 1,2-anhydro sugar intermediate is in a ^4E conformation, in agreement with the X-ray structure of the wild-type enzyme in complex with cyclohexane β-1,2-aziridine (*vide infra*).

To explore other possible mechanisms, we performed simulations with different collective variables. In particular, we quantified whether the canonical Koshland-type mechanism is a viable alternative mechanism for *Bx*GH99. To do so, an additional metadynamics simulation was performed in which the O2 atom was not included in the CV set, thereby excluding any bias toward epoxide formation. Specifically, we considered common CVs used to describe a classical Koshland double displacement reaction (i.e., considering the O_{E333}−C1 and C1−O1 distances as CV1 with the same CV2 as in the previous simulation).[27] The results, shown in the Supporting Information, reveal that even in this case, a double displacement reaction is not favorable; instead E333 acts as a base to abstract a proton from the 2-OH, leading to the same epoxide intermediate (Figure S5). Altogether, our simulations provide computational support for a neighboring-group participation mechanism for *Bx*GH99 *endo*-α-1,2-mannanase.

Structures and Reactivity of Intermediate-Mimicking Complexes. To study the interactions and reactivity of the intermediate, we designed and synthesized compounds that mimic the GH99 Glc/Man-α-1,3-linked β-1,2-anhydrosugar intermediate. To improve their chemical stability, we replaced the endocyclic oxygen with methylene (CH_2), as previous work showed that the affinity of a glycal inhibitor was similar to that of the corresponding cyclohexene.[20] Thus, we synthesized cyclohexane-β-1,2-epoxide **1** and cyclohexane-β-1,2-aziridine **3** (Figure 1c). To demonstrate stereospecificity, and to control for potential promiscuous reactivity of epoxides, we also synthesized the α-isomers: cyclohexane-α-1,2-epoxide **2** and cyclohexane-α-1,2-aziridine **4**.[28]

As reactivity of an intermediate mimic can provide strong evidence for the mechanism, the ability of *Bt*GH99, *Bx*GH99 wild-type, E333Q, and E336Q to catalyze reactions of these

https://dx.doi.org/10.1021/acscentsci.0c00111
ACS Cent. Sci. 2020, 6, 760−770

a

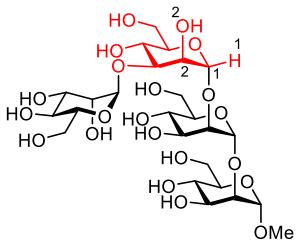

αMan-1,3-αMan-1,2-αMan-1,2-αMan-OMe
[(Man)$_4$OMe]

site of KIE measurement	'light' substrates	'heavy' substrates
H1	(1-^{13}C)	(1-^{2}H,1-^{13}C)
O2	(2-^{13}C)	(2-^{13}C,2-^{18}O)
C1	(2-^{13}C)	(1,2-^{13}C$_2$)

b

	Experimental KIEs	
position	***Bt*GH99 catalyzed (this work)**	**base promoted hydrolysis of PNPMan (Ref.[4])**
1-^{2}H	1.123 ± 0.012	1.112 ± 0.004
1-^{13}C	1.030 ± 0.005	1.026 ± 0.006
2-^{18}O	1.052 ± 0.006	1.044 ± 0.006

c

distance (Å)	**TS structure for *Bx*GH99 hydrolysis of (Man)$_4$OMe**	**TS structure for PNPMan hydrolysis (Ref. [4])**
C1…O1	1.9	2.3
C1…O2	2.3	2.0
O2...O_base	2.7	2.7

Figure 5. Substrate structures and kinetic isotope effect measurements. (a) Structure of substrate and table of isotopologues required for measurement of ^{2}H-, ^{13}C-, and ^{18}O-KIEs. (b) Table of KIEs (±standard error) for the *Bt*GH99-catalyzed hydrolysis of the tetrasaccharide substrate, and published TS distances (±standard error) for the base-promoted hydrolysis of 4-nitrophenyl α-D-mannopyranoside (PNPMan). (c) Calculated critical interatomic distances for the calculated transition states for *Bt*GH99-catalyzed hydrolysis of the tetrasaccharide substrate, and published KIEs for the base-promoted hydrolysis of PNPMan.

compounds was studied by mass spectrometry. The only enzyme-catalyzed reaction observed was for the β-1,2-epoxide **1**, which was converted to an M+18 species (Figure 4, Figure S6); the α-1,2-epoxide **2** and both α- and β-1,2-aziridines, **3** and **4**, were inert (see Figure S7 for data for other compounds). The lack of reactivity of α-1,2-epoxide **2**, which stands in contrast to the reactivity observed for β-1,2-epoxide **1**, is consistent with stereochemical specificity of GH99 enzymes and provides evidence that there is not a nucleophilic enzymatic residue situated "above" the sugar ring. The rate of formation of the M+18 species was linear as a function of time and was proportional to enzyme concentration. Using mass spectrometry the rates of product formation were 0.090 s^{-1} for *Bt*GH99 and 0.047 s^{-1} for *Bx*GH99, in concordance with data showing that GlcManF is turned over more slowly by *Bx*GH99 than *Bt*GH99.[18] ^{1}H NMR spectroscopy of the product of the reaction revealed it to be a vicinal diol with an α-configuration **5** matching that of the product of the endomannanase reaction (Supporting Methods). Thus, the cyclohexane β-1,2-epoxide exhibits reactivity expected for a 1,2-anhydro sugar intermediate, but with a rate of turnover approximately 1/30th of that of Glc−Man fluoride[18] at the same concentration, a result consistent with a lowered reactivity arising from the reduced charge-stabilization at the transition state because of the absence of an endocyclic oxygen. Notably, the α-1,2-epoxide **2** did not react with the GH99 enzyme to yield a covalently labeled enzyme, as might be expected if GH99 enzymes used an enzymatic nucleophile based on similar precedents with variants of cyclophellitol epoxide and its aziridine.[29]

The stability of the β-1,2-aziridine **3** to enzyme action (unlike β-epoxide **1**) enabled the measurement of a binding constant (K_D) of 17.7 ± 1.3 μM for *Bt*GH99 using NMR, as described previously[20] (Figure S8). The 3D structure of aziridine **3** bound to GH99 provides the first structural insight into an intermediate-mimicking complex (Figure 2d). The complex of the wild-type enzyme with the β-1,2-aziridine was obtained at 1.25 Å resolution and subsequently at 1.07 Å for a ternary complex including α-1,2-mannobiose. The −1 pseudosugar is observed in a ^{4}E conformation, as predicted by QM/MM calculations, and consistent with the proposed $^{2}E/^{2}H_3 \rightarrow [E_3]^{\ddagger} \rightarrow {}^{4}E$ conformational itinerary. Within both structures the aziridine N−E333 Oε distance is 2.6 Å, supportive of a role for E333 as acid/base residue.

The greater reactivity of the epoxide species, and its regioselectivity for enzyme-catalyzed ring opening, matches that expected for the putative 1,2-anhydro sugar intermediate and prompted efforts to obtain an epoxide complex with *Bx*GH99. Crystal structures of the cyclohexane β-1,2-epoxide **1** were subsequently obtained with the wild-type and both the E333Q and E336Q mutants, at resolutions of 1.28, 1.12, and 1.34 Å, respectively (Figure 4c). Consistent with the proposed mechanism in which E333 is the base required for epoxide opening, the epoxide remained intact for the E333Q mutant and was opened to the *trans*-1,2-diol **5** with both wild-type and the E336Q mutant. As with the aziridine, the epoxide binds in a ^{4}E conformation, matching the QM/MM calculations. The *trans*-diaxially opened cyclohexanediol was α-configured and in a product-mimicking $^{4}C_1$ conformation. These results confirm

https://dx.doi.org/10.1021/acscentsci.0c00111
ACS Cent. Sci. 2020, 6, 760−770

that the β-1,2-epoxide ring is opened by GH99 yielding an α-configured product, and that the E333 residue is required for this activity. For a direct comparison of the structures of complexes with the intermediate mimics, see Figure S9.

Human *endo*-α-1,2-mannosidase catalyzes glycosylation of α-1,2-mannobiose with retention of stereochemistry using Glc−Man fluoride as donor to yield GlcManManMan, and it is proposed that this reaction proceeds through a 1,2-anhydro sugar intermediate.[22] Incubation of *Bt*GH99 and *Bx*GH99 wild-type enzymes with the β-epoxide **1** and α-1,2-mannobiose yielded a product with mass spectrometric data consistent with a Glc−carbamannose−Man_2 tetrasaccharide (m/z of 883.4 assigned to the permethylated M+Na species detected using MALDI-MS, see Figure S10 and Supporting Methods). The proposed alkylation reaction mechanism is shown in Figure S11.

Kinetic Isotope Effect Analysis of Substrate Cleavage. The foregoing structural and reactivity data with substrate, product, and putative intermediate mimics and the accompanying computational data are collectively consistent with the proposed neighboring-group participation by O2 but do not directly demonstrate the involvement of this residue in the enzymatic mechanism. Kinetic isotope effects (KIEs) are a powerful method to directly study transition state structure as they allow differences in rate of isotope-substituted substrates to report on hybridization, bond order, and geometry changes between the ground and the transition states. Unlike substrate variation studies, KIE studies utilize isotopologues that vary only in the number of neutrons at specific sites and thus constitute a minimal perturbation to the substrate. We recently reported KIEs at six sites (C1, O1, and H1 and C2, O2, and H2) for the alkaline solvolysis of PNPMan, which proceeds through a C2-oxyanion en route to a 1,2-anhydro sugar.[4] Among the most characteristic KIEs were a strikingly large $^{16}O/^{18}O$ KIE for O2 of 1.044 ± 0.006, $^{12}C/^{13}C$ KIEs for C1 of 1.026, and $^{1}H/^{2}H$ KIE for H1 of 1.112 (Figure 5b). These data are supportive of nucleophile participation by an O2 oxyanion, rate-limiting C1−O_{LG} bond cleavage, and an exploded transition state arising from the late build-up in strain of the epoxide of the intermediate. These KIEs represent benchmark data against which to compare KIE data at the equivalent sites for enzymatic cleavage, noting that alkaline solvolysis is a specific base-catalyzed process whereas the enzymatic process is likely to involve both general-acid and general-base catalysis.

Chan et al. reported the development of a highly sensitive competitive NMR method that allows the high-precision measurement of KIEs on milligram quantity mixtures of light and heavy isotopologues each possessing an NMR active probe nucleus (typically ^{13}C) that reported on an adjacent site labeled with light and heavy isotopes.[30] An NMR spectrometer is used to measure competitive KIEs for the second-order rate constant (k_{cat}/K_M) by monitoring reaction mixtures of isotopologue substrates. Owing to redundancies, measurement of KIEs using this technique at the C1, H1, and O2 positions requires just five isotopologues labeled at one or two positions. Prior work showed that simple aryl disaccharides are poor substrates for *Bt* and *Bx*GH99.[12] Thus, we elected to synthesize the tetrasaccharide $(Man)_4OMe$ as a preferred substrate. A reliable 24-step synthesis (13 of which were on isotope-labeled intermediates) was developed and applied for the synthesis of five isotopologues, plus the parent unlabeled tetrasaccharide. Despite its length, the efficiency of this approach allowed conversion of less than 100 mg of isotopically labeled D-mannoses to sufficient amounts of tetrasaccharide for measurement of KIEs using the competitive NMR technique.

KIE measurements were performed by acquisition of quantitative ^{13}C NMR spectra of the *Bt*GH99-catalyzed hydrolysis of mixtures of approximately 1 mg each of the ^{13}C-labeled pair of compounds possessing light or heavy isotopes at the adjacent position (Figure 5a). Due to the presence of a minor ^{13}C-labeled impurity, which was impervious to GH99 catalysis, the spectrum for the reaction at completion was subtracted from the spectra acquired earlier, on the same sample, at varying degrees of completion. Following processing and normalization of data, KIE effects were calculated (Table S3 and Figures S12−S14). The KIE values reveal the $^{1}H/^{2}H$ KIE for H1 of 1.123, $^{12}C/^{13}C$ KIEs for C1 of 1.030, and $^{16}O/^{18}O$ KIE for O2 of 1.052 (Figure 5b). While these KIE measurements are less precise than we would have wished due to the unknown ^{13}C-labeled impurity, they show that there are significant zero-point energy changes at C1 and O2, and these KIE values are clearly consistent with nucleophilic participation by O2 that leads to formation of an epoxide intermediate.

Strikingly, the enzymatic KIE values are essentially identical to that measured for the base-promoted (nonenzymatic) reaction, providing support for a similar transition state structure and reaction mechanism. The anomeric ^{13}C-KIE of 1.030 is in the range associated with S_N2 reactions on glycosides that proceed through "exploded" associative transition states. The α-secondary deuterium KIE for glycosidic bond fission originates mainly from changes in bending vibrations as the anomeric carbon undergoes rehybridization from sp^3 to sp^2 at the transition state. The $^{1}H/^{2}H$ KIE for H1 of 1.123 is smaller than for reactions that proceed through bona fide glycopyranosylium ions, consistent with an exploded S_N2-like transition state, as also predicted by the QM/MM simulations. The nonunity $^{16}O/^{18}O$ KIE of 1.052 for O2 indicates TS involvement of O2 as a nucleophile. The magnitude of this KIE reflects vibrational frequency changes between the ground state and the transition state leading to epoxide formation. For both the enzyme-catalyzed and base-promoted reactions the formation of the three-membered epoxide ring involves the buildup of significant angle strain (~27 kcal/mol),[31] and this results in weakening of the C2−oxygen bond.

At first glance there appears to be a difference between the calculated GH99 TS structure, where epoxide formation occurs after traversal of the TS, and the magnitude of the heavy atom KIEs, which implicate significant motion of the C2-oxygen atom as well as a weakening of the O2−H bond. However, we note that the free energy profile in the vicinity of the transition state (Figure 3a) is relatively flat, and the reaction coordinate includes a shortening of the C1−O2 distance (Figure 3b), which is associated with the C1−C2−O2 bending vibration, as well as a tightening of the O_{E333} to O2 distance, which results in a significant shortening of the distance between H2 and the general-base glutamate, a motion that will also result in zero-point vibrational changes at the labeled O2 site.

Comparisons of the structures calculated for the TS of the enzyme-catalyzed process using QM/MM methods (*vide supra*) and that calculated using *ab initio* methods, calibrated with the KIE measurements, for the hydroxide-promoted hydrolysis of PNPMan[4] provide insights into the structure and

https://dx.doi.org/10.1021/acscentsci.0c00111
ACS Cent. Sci. 2020, 6, 760−770

timing of the respective transition states (Figure 5c). Qualitatively the data (Figure 5c; sum of O2···C1 and C1···O1 distances) suggest similar nucleophile to leaving group distances at the two respective TSs, with that for the specific base-promoted oxyanion being later, and slightly looser, than that for the GH99 *endo*-mannosidase-catalyzed reaction. We conclude that each of the KIE, computational, and structural studies are consistent with this enzyme-catalyzed reaction forming an obligatory epoxide intermediate, and that both theory and experiment (KIE) entail similar, synchronized, heavy atom motions at the TS that are coupled to proton transfer events.

DISCUSSION

Enzyme-catalyzed hydrolytic cleavage of the glycosidic bond can occur through a spectrum of mechanisms that are unified by oxocarbenium ion-like transition states.[1] Reactions that proceed with the retention of configuration involve a two-step reaction with participation by either an enzymic nucleophile (classical retaining glycosidases) or one borne on the substrate (neighboring-group participation glycosidases). The case for neighboring-group participation is convincing for various 2-acetamido-hexosaminidases, where the substrate 2-acetamido group acts as a nucleophile assisting departure of the leaving group and formation of an oxazoline (or oxazolinium ion) intermediate,[32] which is hydrolyzed in the second step.[33] Over 40 years ago, Wallenfels proposed that LacZ β-galactosidase used a mechanism involving nucleophilic participation by a pyranoside 2-hydroxy group to form a 1,2-anhydro sugar (or 1,2-epoxide) intermediate;[34] subsequently this enzyme was shown to utilize a standard retaining mechanism with an enzymatic nucleophile.[7] The present work provides a body of evidence in support of a neighboring-group participation mechanism for GH99 enzymes involving nucleophilic participation by the 2-hydroxyl group and formation of a 1,2-anhydro sugar intermediate, as previously proposed for GH family 99 *endo*-α-1,2-mannosidases/mannanases[18] and recently invoked for α-L-rhamnosidases of GH family 145.[35]

The structures presented here collectively define a series of snapshots along the reaction coordinate of stable molecules that mimic the substrate, intermediate, or product. Comparison of the start and end structures reveals that the key change in these complexes is the shift in the position of the leaving group (O2 of the +1 mannose) as the covalent bond to C1 is cleaved. Computational studies suggest that the conformation of the −1 sugar in the Michaelis complex is perturbed by the very action of making an inactive mutant for X-ray crystallographic study and predicts a $^{2}E/^{2}H_{3}$ conformation. This conformation in the Michaelis complex is unusual for mannosidases, which in all other cases described adopt distorted $^{O}S_{2}$, $^{1}S_{5}$, $^{3}S_{1}$ or $^{1}C_{4}$ conformations that alleviate the steric interaction between the 2-OH and the incoming nucleophile, providing an unfettered nucleophilic trajectory.[36] Notably, in the Michaelis complexes, the −1 subsite sugar adopts a $^{2}E/^{2}H_{3}$ conformation in which the 2-OH sits in between the E333 residue and the anomeric carbon, preventing direct nucleophilic attack at C1, and clearly an alternative strategy must be employed by GH99 enzymes to catalyze glycosidic bond cleavage.

The X-ray structure of the Michaelis complex reveals that the $^{2}E/^{2}H_{3}$ conformation of the −1 mannosyl residue positions O2 in a near-axial orientation, where it is poised to act as an internal nucleophile to displace the anomeric group. Our QM/MM metadynamics simulations show that this leads to a reaction involving nucleophilic attack by O2 on the anomeric carbon, forming a 1,2-anhydro sugar intermediate and excluding the classical Koshland double-displacement mechanism involving an enzymatic nucleophile. As mimics of the highly reactive 1,2-anhydro sugar intermediate, we explored more stable cyclohexane analogues: a β-1,2-epoxide **1** and a β-1,2-aziridine **3**. The β-1,2-aziridine **3** proved sufficiently stable to allow acquisition of a complex with *Bx*GH99 (and with the β-1,2-epoxide for a catalytically disabled mutant), providing insight into the conformation of a 1,2-anhydro sugar mimic. Both complexes gave evidence for the 1,2-anhydro sugar intermediate binding in a ^{4}E conformation, as predicted computationally, and showed the proposed catalytic machinery E333 and E336 positioned appropriately to assist nucleophilic attack by water and provide general acid catalysis to open the ring.

The cyclohexane β- and α-1,2-epoxides **1** and **2** exhibit reactivity that suggests that only the former acts as a bona fide mimic of the proposed 1,2-anhydro sugar intermediate. In particular, only **1** was a substrate for *Bt*GH99 and underwent regioselective hydrolysis at the position equivalent to the anomeric position, to give a 1,2-*trans* product **5**. The reactivity profile of β-1,2-epoxide **1** extends to reaction with 1,2-α-mannobiose, which yielded a pseudotetrasaccharide, a reaction analogous to the transglycosylation reaction of *Hs*GH99 using GlcManF with 1,2-α-mannobiose,[22] recapitulating the reactivity invoked for the 1,2-anhydrosugar intermediate.

Kinetic isotope effects are considered the gold standard for experimental investigations of transition state structure. Using a highly sensitive competitive NMR method we measured α-secondary KIEs for $^{1}H/^{2}H$ for H1 of 1.123 ± 0.012 and for $^{12}C/^{13}C$ of 1.030 ± 0.005, and a $^{16}O/^{18}O$ KIE for O2 of 1.052 ± 0.006. The α-secondary deuterium and primary anomeric ^{13}C-KIEs are consistent with that expected for a reaction center undergoing $sp^{3} \rightarrow sp^{2}$ rehybridization at the TS such as that which occurs in an exploded $S_{N}2$-type reaction. In addition, the $^{16}O/^{18}O$ KIE indicates a primary KIE associated with O2 acting as a nucleophile at the experimentally observed TS. These KIEs are essentially identical to benchmark KIEs determined for the hydroxide-promoted hydrolysis of 4-nitrophenyl α-mannoside[4] (although are consistent with an earlier, looser transition state) and provide direct evidence for neighboring-group participation by *Bx*GH99.

CONCLUSIONS

Collectively the 3D structures, QM/MM calculations, KIE measurements, and the reactivity of cyclohexane epoxide intermediate mimics provide evidence that GH99 enzymes achieve substitution with retention of stereochemistry through a neighboring-group participation mechanism by O2 involving general base-assistance by E333 and leading to a 1,2-anhydro sugar intermediate, via a TS with oxocarbenium ion character. 3D structures and QM/MM calculations are consistent with the enzyme achieving this outcome through a conformational itinerary along the reaction coordinate of $^{2}H_{3} \rightarrow [E_{3}]^{\ddagger} \rightarrow {}^{4}E$. This conformational pathway is distinct from that used by all other characterized mannosidases as it involves only minor distortion of the −1 sugar residue at the Michaelis complex, whereas pathways involving $^{3}H_{4}$ and $B_{2,5}$ transition state conformations require substantial distortion to alleviate nucleophile···O2 interactions. This work provides strong

https://dx.doi.org/10.1021/acscentsci.0c00111
ACS Cent. Sci. 2020, 6, 760−770

evidence for the existence of a 1,2-anhydro sugar mechanism in biological catalysis that is broadly equivalent to the 1,2-anhydro sugars that have long been implicated as intermediates in the base-promoted hydrolysis of *trans*-1,2-glycosides.

■ ASSOCIATED CONTENT

Supporting Information

The Supporting Information is available free of charge at https://pubs.acs.org/doi/10.1021/acscentsci.0c00111.

Methods describing protein crystallography, computational methods, enzymatic reactions, and MS and NMR analysis of products, KIE measurements, synthetic methods and characterization data for synthesis of cyclohexane epoxides and aziridines, and of isotopologues used for KIE studies, and NMR spectra for new compounds (PDF)

Additional data and figures including X-ray data, bond lengths, KIEs, structures, conformational states, mass spectrometry data, NMR titration results, thin layer chromatography, and mechanisms (PDF)

Accession Codes

The coordinates and structure factors have been deposited in the Protein Data Bank (accession codes 6FWG, 6FWI, 6FWJ, 6FWL, 6FWM, 6FWO, 6FWP, and 6FWQ).

■ AUTHOR INFORMATION

Corresponding Authors

Andrew J. Bennet − *Department of Chemistry and Department of Biochemistry and Molecular Biology, Simon Fraser University, Burnaby, British Columbia V5A 1S6, Canada;* orcid.org/0000-0002-8378-6752; Email: bennet@sfu.ca

Matthieu Sollogoub − *Sorbonne Université, CNRS, Institut Parisien de Chimie Moléculaire, UMR 8232, 75005 Paris, France;* orcid.org/0000-0003-0500-5946; Email: matthieu.sollogoub@sorbonne-universite.fr

Carme Rovira − *Departament de Química Inorgànica i Orgànica (Secció de Química Orgànica) & Institut de Química Teòrica i Computacional (IQTCUB), Universitat de Barcelona, 08028 Barcelona, Spain; Institució Catalana de Recerca i Estudis Avançats (ICREA), 08010 Barcelona, Spain;* orcid.org/0000-0003-1477-5010; Email: c.rovira@ub.edu

Gideon J. Davies − *York Structural Biology Laboratory, Department of Chemistry, University of York, York YO10 5DD, United Kingdom;* orcid.org/0000-0002-7343-776X; Email: gideon.davies@york.ac.uk

Spencer J. Williams − *School of Chemistry and Bio21 Molecular Science and Biotechnology Institute, University of Melbourne, Parkville, Victoria 3010, Australia;* orcid.org/0000-0001-6341-4364; Email: sjwill@unimelb.edu.au

Authors

Lukasz F. Sobala − *York Structural Biology Laboratory, Department of Chemistry, University of York, York YO10 5DD, United Kingdom*

Gaetano Speciale − *School of Chemistry and Bio21 Molecular Science and Biotechnology Institute, University of Melbourne, Parkville, Victoria 3010, Australia*

Sha Zhu − *Sorbonne Université, CNRS, Institut Parisien de Chimie Moléculaire, UMR 8232, 75005 Paris, France*

Lluís Raich − *Departament de Química Inorgànica i Orgànica (Secció de Química Orgànica) & Institut de Química Teòrica i Computacional (IQTCUB), Universitat de Barcelona, 08028 Barcelona, Spain*

Natalia Sannikova − *Department of Chemistry, Simon Fraser University, Burnaby, British Columbia V5A 1S6, Canada*

Andrew J. Thompson − *York Structural Biology Laboratory, Department of Chemistry, University of York, York YO10 5DD, United Kingdom;* orcid.org/0000-0001-7865-1856

Zalihe Hakki − *School of Chemistry and Bio21 Molecular Science and Biotechnology Institute, University of Melbourne, Parkville, Victoria 3010, Australia*

Dan Lu − *Sorbonne Université, CNRS, Institut Parisien de Chimie Moléculaire, UMR 8232, 75005 Paris, France*

Saeideh Shamsi Kazem Abadi − *Department of Biochemistry and Molecular Biology, Simon Fraser University, Burnaby, British Columbia V5A 1S6, Canada*

Andrew R. Lewis − *Department of Chemistry, Simon Fraser University, Burnaby, British Columbia V5A 1S6, Canada*

Víctor Rojas-Cervellera − *Departament de Química Inorgànica i Orgànica (Secció de Química Orgànica) & Institut de Química Teòrica i Computacional (IQTCUB), Universitat de Barcelona, 08028 Barcelona, Spain*

Ganeko Bernardo-Seisdedos − *Molecular Recognition and Host−Pathogen Interactions, CIC bioGUNE, Basque Research Technology Alliance (BRTA), 48160 Derio, Spain*

Yongmin Zhang − *Sorbonne Université, CNRS, Institut Parisien de Chimie Moléculaire, UMR 8232, 75005 Paris, France*

Oscar Millet − *Molecular Recognition and Host−Pathogen Interactions, CIC bioGUNE, Basque Research Technology Alliance (BRTA), 48160 Derio, Spain;* orcid.org/0000-0001-8748-4105

Jesús Jiménez-Barbero − *Ikerbasque, Basque Foundation for Science, 48013 Bilbao, Spain; Molecular Recognition and Host−Pathogen Interactions, CIC bioGUNE, Basque Research Technology Alliance (BRTA), 48160 Derio, Spain;* orcid.org/0000-0001-5421-8513

Complete contact information is available at: https://pubs.acs.org/10.1021/acscentsci.0c00111

Author Contributions

¶L.F.S., G.S., S.Z., and L.R. contributed equally. G.J.D. and S.J.W. conceived the project. C.R., M.S., A.J.B., G.J.D., and S.J.W. designed the experiments. G.S., Z.H., D.L., S.Z., and Y.Z. synthesized ligands and substrates. N.S., S.S.K.A., A.R.L., and A.J.B. measured KIEs and analyzed results. L.F.S., A.J.T., Z.H., and G.J.D. conducted X-ray crystallography and analyzed results. L.F.S. and S.Z. performed enzymatic reactions and analyzed results. G.B.-S., L.F.S., O.M., and J.J.-B. performed NMR measurements of ligand affinities. L.R., V.R.-C., and C.R. performed computational studies. C.R., A.J.B., G.J.D., and S.J.W. wrote the manuscript with input from other authors.

Notes

The authors declare no competing financial interest.

■ ACKNOWLEDGMENTS

This work was supported by the Australian Research Council (FT130100103, DP120101396, DP180101957), the BBSRC (A.J.T.), European Research Council (ERC-2012-AdG-322942 "Glycopoise"; L.F.S.), Natural Sciences and Engineering Research Council of Canada (A.J.B. Discovery Grant: 2017-04910), the Spanish Ministry of Science, Innovation and Universities (MICINN/AEI/FEDER) (CTQ2017-85496-P to C.R.), the Spanish Structures of Excellence María de Maeztu

(MDM-2017-0767 to C.R.), and the Agency for Management of University and Research Grants of Generalitat de Catalunya (AGAUR) (2017SGR-1189 to C.R.). G.J.D. is funded by the Royal Society "Ken Murray" Professorship. We are grateful to Sivanandam Veeramuthu for help with NMR. We thank Diamond Light Source for access to beamlines I02, I04, and I04-1 (proposals mx-9948 and mx-13587). In-house crystal screening was performed on X-ray equipment provided, in part, by the Wellcome Trust. The authors gratefully acknowledge the computer resources and technical support provided by the Barcelona Supercomputing Center (BSC−CNS, Barcelona, Spain). The group at Bilbao thanks the Agencia Estatal de Investigacion of Spain (Grants RTI2018-101269-B-I00 and RTI2018-094751-B-C21), the European Research Council (RECGLYCANMR, ERC AdG 788143), and the Severo Ochoa Excellence accreditation (SEV2016-0644).

REFERENCES

(1) Sinnott, M. L. Catalytic mechanisms of enzymatic glycosyl transfer. *Chem. Rev.* **1990**, *90*, 1171−1202.
(2) Gasman, R. C.; Johnson, D. C. C-2 Oxyanion Participation in the Base-Catalyzed Cleavage of p-Nitrophenyl β-D-Galactopyranoside and p-Nitrophenyl α-D-Mannopyranoside. *J. Org. Chem.* **1966**, *31*, 1830−1838.
(3) Micheel, F.; Borrmann, D. Ein neues Verfahren zur Synthese höherer Saccharide. *Chem. Ber.* **1960**, *93*, 1143−1147.
(4) Speciale, G.; Farren-Dai, M.; Shidmoossavee, F. S.; Williams, S. J.; Bennet, A. J. C2-Oxyanion neighboring group participation: Transition state structure for the hydroxide-promoted hydrolysis of 4-nitrophenyl α-D-mannopyranoside. *J. Am. Chem. Soc.* **2016**, *138*, 14012−14019.
(5) Brockhaus, M.; Dettinger, H.-M.; Kurz, G.; Lehmann, J.; Wallenfels, K. Participation of HO-2 in the cleavage of β-D-galactosides by the β-D-galactosidase from *E. coli*. *Carbohydr. Res.* **1979**, *69*, 264−268.
(6) Johnson, R. W.; Marschner, T. M.; Oppenheimer, N. J. Pyridine nucleotide chemistry. A new mechanism for the hydroxide-catalyzed hydrolysis of the nicotinamide-glycosyl bond. *J. Am. Chem. Soc.* **1988**, *110*, 2257−2263.
(7) Gebler, J. C.; Aebersold, R.; Withers, S. G. Glu-537, not Glu-461, is the nucleophile in the active site of (lac Z) β-galactosidase from *Escherichia coli*. *J. Biol. Chem.* **1992**, *267*, 11126−11130.
(8) Egea, P. F.; Muller-Steffner, H.; Kuhn, I.; Cakir-Kiefer, C.; Oppenheimer, N. J.; Stroud, R. M.; Kellenberger, E.; Schuber, F. Insights into the Mechanism of Bovine CD38/NAD$^+$ Glycohydrolase from the X-Ray Structures of Its Michaelis Complex and Covalently-Trapped Intermediates. *PLoS One* **2012**, *7*, e34918.
(9) Handlon, A. L.; Xu, C.; Muller-Steffner, H. M.; Schuber, F.; Oppenheimer, N. J. 2′-Ribose Substituent Effects on the Chemical and Enzymic Hydrolysis of NAD+. *J. Am. Chem. Soc.* **1994**, *116*, 12087−12088.
(10) Lombard, V.; Golaconda Ramulu, H.; Drula, E.; Coutinho, P. M.; Henrissat, B. The carbohydrate-active enzymes database (CAZy) in 2013. *Nucleic Acids Res.* **2014**, *42*, D490−5.
(11) Ten years of CAZypedia: a living encyclopedia of carbohydrate-active enzymes. *Glycobiology* **2018**, *28*, 3−8. DOI: 10.1093/glycob/cwx089.
(12) Hakki, Z.; Thompson, A. J.; Bellmaine, S.; Speciale, G.; Davies, G. J.; Williams, S. J. Structural and kinetic dissection of the *endo*-α-1,2-mannanase activity of bacterial GH99 glycoside hydrolases from *Bacteroides* spp. *Chem. - Eur. J.* **2015**, *21*, 1966−77.
(13) Lubas, W. A.; Spiro, R. G. Evaluation of the role of rat liver Golgi endo-α-D-mannosidase in processing N-linked oligosaccharides. *J. Biol. Chem.* **1988**, *263*, 3990−3998.
(14) Moore, S. E.; Spiro, R. G. Demonstration that Golgi endo-α-D-mannosidase provides a glucosidase-independent pathway for the formation of complex N-linked oligosaccharides of glycoproteins. *J. Biol. Chem.* **1990**, *265*, 13104−13112.
(15) Moore, S. E.; Spiro, R. G. Characterization of the endomannosidase pathway for the processing of N-linked oligosaccharides in glucosidase II-deficient and parent mouse lymphoma cells. *J. Biol. Chem.* **1992**, *267*, 8443−8451.
(16) Cuskin, F.; Lowe, E. C.; Temple, M. J.; Zhu, Y.; Cameron, E. A.; Pudlo, N. A.; Porter, N. T.; Urs, K.; Thompson, A. J.; Cartmell, A.; Rogowski, A.; Hamilton, B. S.; Chen, R.; Tolbert, T. J.; Piens, K.; Bracke, D.; Vervecken, W.; Hakki, Z.; Speciale, G.; Munoz-Munoz, J. L.; Day, A.; Pena, M. J.; McLean, R.; Suits, M. D.; Boraston, A. B.; Atherly, T.; Ziemer, C. J.; Williams, S. J.; Davies, G. J.; Abbott, D. W.; Martens, E. C.; Gilbert, H. J. Human gut Bacteroidetes can utilize yeast mannan through a selfish mechanism. *Nature* **2015**, *517*, 165−169.
(17) Roth, J.; Ziak, M.; Zuber, C. The role of glucosidase II and endomannosidase in glucose trimming of asparagine-linked oligosaccharides. *Biochimie* **2003**, *85*, 287−94.
(18) Thompson, A. J.; Williams, R. J.; Hakki, Z.; Alonzi, D. S.; Wennekes, T.; Gloster, T. M.; Songsrirote, K.; Thomas-Oates, J. E.; Wrodnigg, T. M.; Spreitz, J.; Stutz, A. E.; Butters, T. D.; Williams, S. J.; Davies, G. J. Structural and mechanistic insight into N-glycan processing by endo-α-mannosidase. *Proc. Natl. Acad. Sci. U. S. A.* **2012**, *109*, 781−786.
(19) Fernandes, P. Z.; Petricevic, M.; Sobala, L.; Davies, G. J.; Williams, S. J. Exploration of Strategies for Mechanism-Based Inhibitor Design for Family GH99 endo-α-1,2-Mannanases. *Chem. - Eur. J.* **2018**, *24*, 7464−7473.
(20) Petricevic, M.; Sobala, L. F.; Fernandes, P.; Raich, L.; Thompson, A. J.; Bernardo-Seisdedos, G.; Millet, O.; Zhu, S.; Sollogoub, M.; Jimenez-Barbero, J.; Rovira, C.; Davies, G. J.; Williams, S. J. Contribution of shape and charge to the inhibition of a family GH99 *endo*-α-1,2-mannanase. *J. Am. Chem. Soc.* **2017**, *139*, 1089−1097.
(21) Davies, G. J.; Wilson, K. S.; Henrissat, B. Nomenclature for sugar-binding subsites in glycosyl hydrolases. *Biochem. J.* **1997**, *321*, 557−559.
(22) Iwamoto, S.; Kasahara, Y.; Yoshimura, Y.; Seko, A.; Takeda, Y.; Ito, Y.; Totani, K.; Matsuo, I. Endo-alpha-Mannosidase-Catalyzed Transglycosylation. *ChemBioChem* **2017**, *18*, 1376−1378.
(23) Barducci, A.; Bonomi, M.; Parrinello, M. Metadynamics. *Wiley Interdiscip. Rev.: Comput. Mol. Sci.* **2011**, *1*, 826−843.
(24) Laio, A.; Parrinello, M. Escaping free-energy minima. *Proc. Natl. Acad. Sci. U. S. A.* **2002**, *99*, 12562−12566.
(25) Ardèvol, A.; Rovira, C. Reaction Mechanisms in Carbohydrate-Active Enzymes: Glycoside Hydrolases and Glycosyltransferases. Insights from ab Initio Quantum Mechanics/Molecular Mechanics Dynamic Simulations. *J. Am. Chem. Soc.* **2015**, *137*, 7528−7547.
(26) Petersen, L.; Ardevol, A.; Rovira, C.; Reilly, P. J. Molecular mechanism of the glycosylation step catalyzed by Golgi α-mannosidase II: a QM/MM metadynamics investigation. *J. Am. Chem. Soc.* **2010**, *132*, 8291−8300.
(27) Biarnés, X.; Ardèvol, A.; Iglesias-Fernández, J.; Planas, A.; Rovira, C. Catalytic Itinerary in 1,3−1,4-β-Glucanase Unraveled by QM/MM Metadynamics. Charge Is Not Yet Fully Developed at the Oxocarbenium Ion-like Transition State. *J. Am. Chem. Soc.* **2011**, *133*, 20301−20309.
(28) Lu, D.; Zhu, S.; Sobala, L. F.; Bernardo-Seisdedos, G.; Millet, O.; Zhang, Y.; Jiménez-Barbero, J.; Davies, G. J.; Sollogoub, M. From 1,4-Disaccharide to 1,3-Glycosyl Carbasugar: Synthesis of a Bespoke Inhibitor of Family GH99 Endo-α-mannosidase. *Org. Lett.* **2018**, *20*, 7488−7492.
(29) Wu, L.; Armstrong, Z.; Schroder, S. P.; de Boer, C.; Artola, M.; Aerts, J. M.; Overkleeft, H. S.; Davies, G. J. An overview of activity-based probes for glycosidases. *Curr. Opin. Chem. Biol.* **2019**, *53*, 25−36.
(30) Chan, J.; Lewis, A. R.; Gilbert, M.; Karwaski, M. F.; Bennet, A. J. A direct NMR method for the measurement of competitive kinetic isotope effects. *Nat. Chem. Biol.* **2010**, *6*, 405−7.

(31) Whalen, D. L. Mechanisms of hydrolysis and rearrangements of epoxides. *Adv. Phys. Org. Chem.* **2005**, *40*, 247−298.
(32) Coines, J.; Alfonso-Prieto, M.; Biarnés, X.; Planas, A.; Rovira, C. Oxazoline or Oxazolinium Ion? The Protonation State and Conformation of the Reaction Intermediate of Chitinase Enzymes Revisited. *Chem. - Eur. J.* **2018**, *24*, 19258−19265.
(33) Macauley, M. S.; Whitworth, G. E.; Debowski, A. W.; Chin, D.; Vocadlo, D. J. O-GlcNAcase uses substrate-assisted catalysis: kinetic analysis and development of highly selective mechanism-inspired inhibitors. *J. Biol. Chem.* **2005**, *280*, 25313−22.
(34) Wallenfels, K.; Weil, R. In *The Enzymes*, 3rd ed.; Boxer, P. D., Ed.; Academic Press: New York, 1972; Vol. *7*, pp 617−663.
(35) Munoz-Munoz, J.; Cartmell, A.; Terrapon, N.; Henrissat, B.; Gilbert, H. J. Unusual active site location and catalytic apparatus in a glycoside hydrolase family. *Proc. Natl. Acad. Sci. U. S. A.* **2017**, *114*, 4936−4941.
(36) Davies, G. J.; Planas, A.; Rovira, C. Conformational analyses of the reaction coordinate of glycosidases. *Acc. Chem. Res.* **2012**, *45*, 308−316.

https://dx.doi.org/10.1021/acscentsci.0c00111
ACS Cent. Sci. 2020, 6, 760−770